Measuring bidirectional reflectance distribution of low reflectivity surfaces in the near infrared

Luan C. Doan, J. Robert Mahan, Kory J. Priestley, Nguyen Q. Vinh

Luan C. Doan, J. Robert Mahan, Kory J. Priestley, Nguyen Q. Vinh, "Measuring bidirectional reflectance distribution of low reflectivity surfaces in the near infrared," Proc. SPIE 11103, Optical Modeling and System Alignment, 111030I (11 September 2019); doi: 10.1117/12.2529629

Event: SPIE Optical Engineering + Applications, 2019, San Diego, California, United States

Measuring Bidirectional Reflectance Distribution of Low Reflectivity Surfaces in the Near Infrared

Luan C. Doan,[1,2] J. Robert Mahan,[2] Kory J. Priestley,[3] and Nguyen Q. Vinh[1]*

[1] Department of Physics and Center for Soft Matter and Biological Physics, Virginia Tech, Blacksburg, VA 24061, USA

2 Department of Mechanical Engineering, Virginia Polytechnic Institute and State University, Blacksburg, VA 24061, USA

[3] Climate Sciences Branch, NASA Langley Research Center, Hampton, Virginia 23682, USA

* Corresponding author: vinh@vt.edu; phone: 1-540-231-3158

ABSTRACT

Knowledge of bidirectional reflectance angular distribution of low reflectivity surfaces is important for predicting stray light in optical systems. We have performed bidirectional reflectance distribution measurements at wavelengths of 633 nm and 850 nm for surfaces coated with Z302, a commercial optical coating material widely used in optical instruments. The bidirectional reflectance properties of these surfaces depend on surface topology characterized by thickness and roughness parameters. To explain our results, we have employed directional scatter analysis of the experimental data that can be represented by a linear combination of diffuse, glossy, and specular, components. Modeling the bidirectional reflectance distribution in the context of a ray-trace can provide important information of stray light, coated surfaces, and their impact on performance of optical instruments.

Keywords: Bidirectional Reflectometry, Bidirectional Reflectance Distribution, Low Reflectivity Surfaces, Near Infrared

1. INTRODUCTION

Black materials with low reflectivity have wide applications in optics, radiation heat transfer, energy conversion, radiometers and bolometers, calibration standards and light trappers in optical systems. Optical engineers select a special material for their black coating when attempting to reduce stray light in an optical instrument [1-3]. The optical properties of these coated materials can be determined by many parameters including optical constants and conditions of the coated surface such as roughness, granularity, and treatment. For example, the black coated layers in well-sealed tubes are critical to the performance of cameras, telescopes, and spectrometers. Aeroglaze® Z302 (Lord) absorptive polyurethane paint [4] is the coating of choice for many optical and aerospace applications where a surface must be an exceptionally efficient absorber. While the material is widely used in many applications, the optical properties as well as the performance of Z302 on the surface of an actual device such as a camera or a telescope has not been extensively documented in the literature. The bidirectional reflectance properties of this material has been reported in a specific wavelength [5-7], and measurement-based models have been employed to simulate the performance of optical devices [2, 8-12]. Needed is more information of bidirectional reflectance properties of the material in different wavelengths. In this paper we explore the optical properties of the Z302 coatings at of wavelengths of 633 nm and 850 nm. Specifically, we employ a semi-empirical method to characterize the bidirectional reflectance of the low reflectivity material coated on a flat silicon surface.

The interaction of radiation with a surface, including specular and diffuse components of reflection, can be expressed as a single function, called the bidirectional reflectance distribution function (BRDF). This is a function of two incident and two reflected angles as well as the wavelength and polarization of the incident radiation. In the spherical coordinate system in Figure 1, the monochromatic BRDF, is defined [11]

$$\mathrm{BRDF} = f_\mathrm{r}(\lambda, \theta_\mathrm{i}, \phi_\mathrm{i}, \theta_\mathrm{r}, \phi_\mathrm{r}) = \frac{\mathrm{d}I_\mathrm{r}(\lambda,\theta_\mathrm{i},\phi_\mathrm{i},\theta_\mathrm{r},\phi_\mathrm{r})}{I_\mathrm{i}(\lambda,\theta_\mathrm{i},\phi_\mathrm{i})\cos\theta_\mathrm{r}\,\mathrm{d}\omega_\mathrm{r}}, \quad (1)$$

Optical Modeling and System Alignment, edited by Mark A. Kahan, José Sasián,
Richard N. Youngworth, Proc. of SPIE Vol. 11103, 111030I · © 2019 SPIE
CCC code: 0277-786X/19/$21 · doi: 10.1117/12.2529629

where dI_r is the differential reflected radiance from a plane surface (W/m^2·sr), I_i is the incident radiance onto the plane surface (W/m^2·sr), θ_i is the polar angle of the incident light, ϕ_i is the azimuthal angle of the incident light, θ_r is the polar angle of the reflected light, ϕ_r is the azimuthal angle of the reflected light, and $d\omega_r$ is the differential solid angle (sr). The BRDF is often referred to as the monochromatic bidirectional reflectivity. The BRDF is important because it includes all information needed to compute the other surface optical properties.

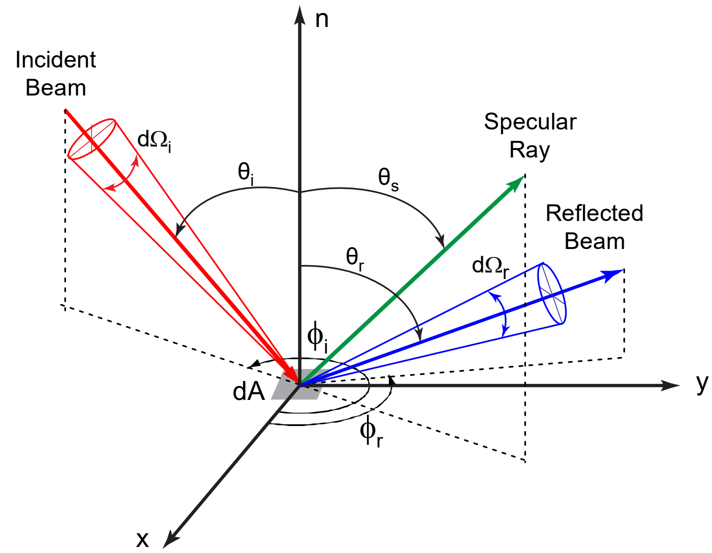

Figure 1. Beams of monochromatic light incident to and reflected from an area element dA.

2. SAMPLE FABRICATION AND EXPERIMENTAL APPARATUS

Z302 samples were prepared by spray-coating or dipping silicon wafers into the Z302 material. We used polished silicon wafers with 500-μm thickness as the substrate of the sample. The surface of the bare silicon wafers was ultra-flat. Thus, these silicon substrates do not produce any relief patterning of the surface of Z302 layers. During spray-coating the Z302 layers were applied by hand-spraying using an air brush. We can vary the thickness of the Z302 layers by performing a different number of re-coats to each sample. For the dipping method, silicon wafers were submerged into the can of liquid Z302 and maintained horizontal during drying process. A thick and extremely smooth surface of these samples can be obtained with a single dipping. A detailed description of the sample preparation has been reported previously [6, 7].

Our measurement setup is based on a classical BRDF gonio-reflectometer [6, 13, 14]. Photos of the gonio-reflectometer setup and the Z302 sample appear in Figure 2, while Figure 3 provides a schematic diagram of the system. The gonio-reflectometer allows coaxial rotation using two precision rotation stages that are controlled using LabVIEW. The rotation stages (Thorlabs - PRM1Z8) controlled by the step motors have high accuracy, resolution, and repeatability. In this setup, the illuminating laser source is stationary. To vary the incidence angle of the sample, the first stage rotates the sample holder around the main axis. The second stage turns the detector to the desired viewing angle position in the plane of incidence, as indicated in the Figure 3. Adapter rings are employed to assure proper alignment.

The Z302 sample is illuminated by a He-Ne laser operating at 633 nm or a tunable wavelength Ti-Sapphire laser with the wavelength range from 750 nm to 850 nm. The *s* or *p*- polarization of these lasers is controlled by a zero-order half-wave plate and a polarizing beam-splitter cube. The laser beam is focused at the center of the Z302 samples. A chopper is employed to modulate the intensity of the laser beam. The frequency of the chopper at 41 Hz was chosen to eliminate the effects of noise and ambient light fluctuations. The scattered light from the surface of Z302 samples is incident to a 200-μm slit mounted on the entrance aperture of a Newport 918-UV photodetector (for UV to near infrared light detection). The area of the slit determines the solid angle of our measurements. Low-noise operation is assured by passing the signal from the detector output successively through a preamplifier and a lock-in amplifier.

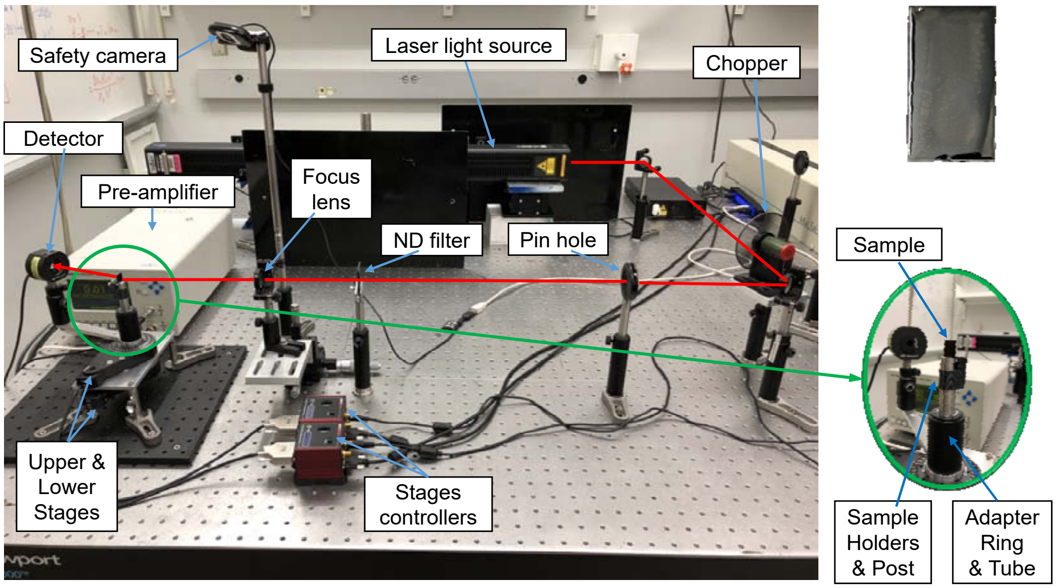

Figure 2. (left) A photo of the bidirectional gonio-reflectometer setup showing an optical table with a laser light source, an optical chopper, mirrors, a pin hole, a neutral density filter, stage controllers, stages, a sample holder, a detector, and a pre-amplifier, and (right) a Z302 sample used in the BRDF experiments.

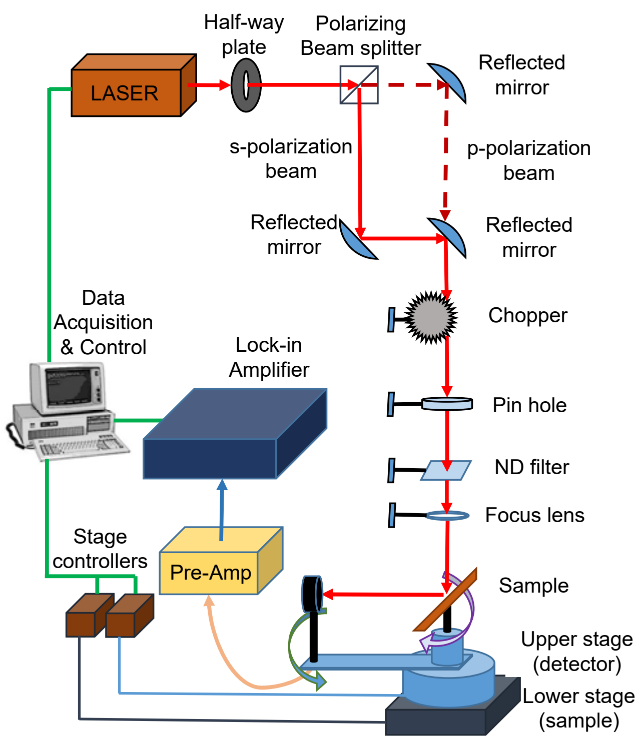

Figure 3. Schematic diagram of the BRDF experimental setup.

3. RESULTS AND DISCUSSION

The BRDF results for the Z302 sample were measured at different incidence angles for illumination wavelengths of 633 nm and 850 nm. The incidence angles can be varied from 10 to 85 deg. The in-plane measured BRDFs at λ = 633 nm are plotted in Figures 4 for both *s*- and *p*-polarizations, and at λ = 850 nm in Figures 5 for *s*-polarizations. To assist comparison, the ordinates have the same scale in both figures. The scattered light from the surface of the Z302 absorber layers became visible at viewing angles near the specular peaks. Therefore, we collected data for viewing angles, θ_r, within a limited range surrounding the direction of specular reflection. Viewing angle intervals of 0.5, 0.2, and 0.05 deg are used near the specular reflection angle, while 5-deg intervals are used for off-specular angles. To reduce random error, the reflection intensity has been averaged over three observations for each viewing angle. Near the specular peaks the standard deviation was observed to be within $\pm$5 percent, while for very small BRDF values the standard deviation was as large as $\pm$30 percent due to the low signal-to-noise ratio. The peak of the BRDFs observed for the s-polarization increases with increasing incidence angle. This trend has already been reported for the UV and visible illumination light [6] and also has been observed for naturally polarized light [11]. The maximum of the BRDFs for *p*-polarized light show a dip at the Brewster angle – about 60 deg in both cases, which is anticipated by classical optics [15]. This observation is consistent with Fresnel reflection from a smooth interface.

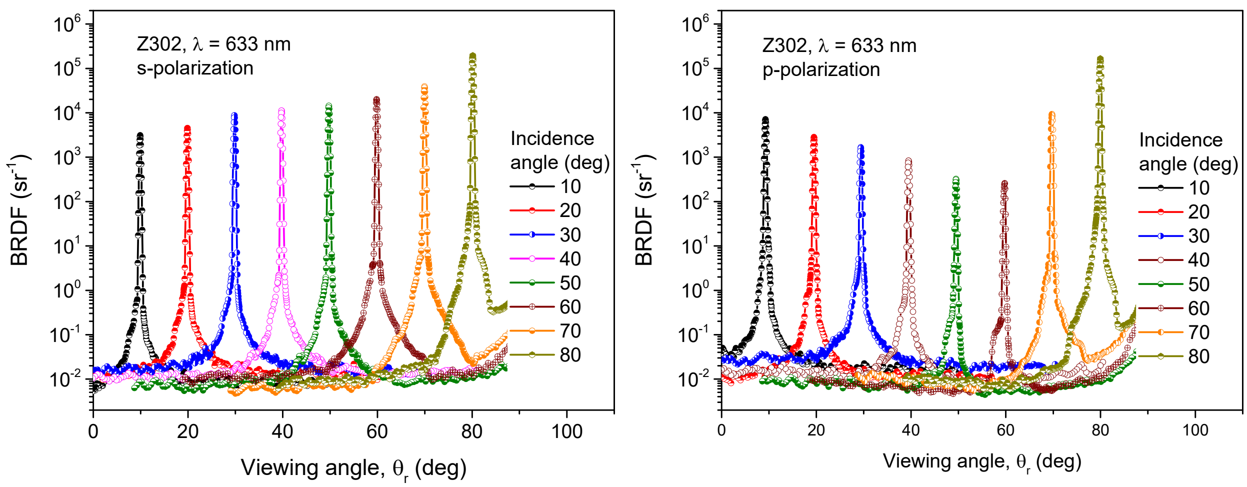

Figure 4. Measured BRDF results obtained at 633 nm at incident angles of from 10 to 80 deg for both (left) *s*- polarization and (right) *p*- polarization.

To characterize the directional scatter of the low reflectivity the Z302 surface, a BRDF model is needed that accurately mimics the observed BRDF behavior of the material as a function of wavelength, incidence, and reflected (viewing) angles. The measured BRDFs for the Z302 sample contain a sharp peak and a broader base, which is a typical bidirectional reflection behavior and thus can be explained using scattering models. The material can be described as being "specular," "glossy," and "diffuse". We use a phenomenological approach to explain the experimental results. Analysis of the available experimental data shows that the BRDF, f_r, can be represented by a linear combination of a diffuse, $f_{r,d}$, a glossy, $f_{r,g}$, and a specular, $f_{r,s}$, component [2]; i.e.,

$$f_r = k_d f_{r,d} + k_s f_{r,s} + k_g f_{r,g}, \tag{2}$$

where k_d, k_s, and k_g are nonnegative values and $k_d + k_s + k_g = 1$. The BRDF model must obey the energy conservation law. This means that the directional-hemispherical reflectance (DHR), ρ, which is defined as the ratio of the power leaving a surface to the power incident upon a surface, has a range limited to $0 \leq \rho \leq 1$ for any incidence angle θ_i; i.e.,

$$\rho(\theta_i) = \int_{2\pi} f_r(\lambda, \theta_i, \phi_i, \theta_r, \phi_r) d\Omega_r \tag{3}$$

where $d\Omega_r = \sin\theta_r \cos\theta_r \, d\theta_r \, d\phi_r$ is the projected solid reflected angle.

The diffuse component corresponds to radiation reflected uniformly within the hemispherical solid angle. The ideal diffuse reflection, known as Lambertian reflection, can be used for the diffuse reflection when $f_{r,d}$ is constant; i.e.,

$$f_{r,d} = \frac{R_d}{\pi}, \tag{4}$$

where R_d is the diffuse reflection constant.

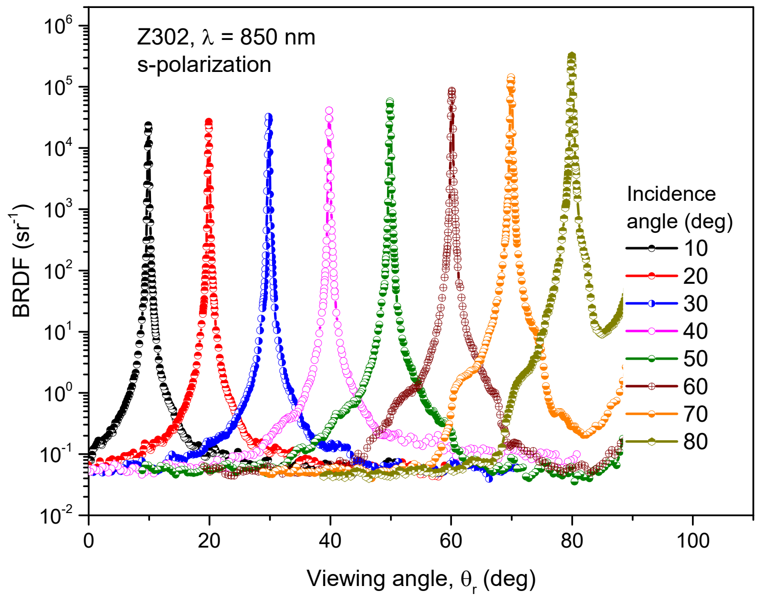

Figure 5. BRDFs measured at 850 nm for *s*- polarization.

For the specular and glossy components, the BRDF results can be explained with scattering models. An unlimited number of BRDF models are available, derived by many researchers attempting to interpret phenomena in their specific areas of interest. Our purpose is to investigate the BRDF behavior of Z302 as a function of wavelength, incidence angle, and viewing angle. The K-correlation is the most suitable approach to accomplish this. In this model, the projected vectors in the scattered and specular directions are defined $\vec{\beta} = \vec{r_r}\sin\theta_r$; $\vec{\beta_0} = \vec{r_0}\sin\theta_0$, where $\vec{\beta}$ and $\vec{\beta_0}$ indicate the vectors in the scatter and specular reflection directions. The angles θ_r and θ_0 are the scatter and specular angles, respectively. These are measured relative to the surface normal. The vectors $\vec{r_r}$ and $\vec{r_0}$ are the incident and specular light rays. Thus, the K-correlation model, used to simulate the BRDFs for a smooth surface ($\hat{\sigma} \ll 1$), can be expressed as a function of $|\vec{\beta} - \vec{\beta_0}|$ [16]; i.e.,

$$BRDF_{\text{K-corr}}(s \neq 2) = \frac{2\pi\, dn^2 RB^2}{\lambda^4} \frac{\sigma^2(\lambda)(s-2)}{(1-(1+(B/\lambda)^2)^{1-s/2})} \frac{\cos\theta_i \cos\theta_r}{(1+B^2(\beta-\beta_0)^2/\lambda^2)}$$

and (5)

$$BRDF_{\text{K-corr}}(s = 2) = \frac{4\pi\, dn^2 RB^2}{\lambda^4} \frac{\sigma^2(\lambda)}{\ln(1+(B/\lambda)^2)} \frac{\cos\theta_i \cos\theta_r}{(1+B^2(\beta-\beta_0)^2/\lambda^2)}.$$

In Eq. (5), λ is the measurement wavelength, s is the slope of BRDF at large spatial frequencies, $B = 2\pi L_c$ in which L_c is the surface correlation length, $\sigma(\lambda)$ is the total effective rms roughness over the frequency range, R is the surface specular reflectivity, and *dn* is the change in the refractive index at the surface (*dn* = 2 for mirror).

The measured BRDFs for the Z302 sample can be fitted with a combination of a diffuse reflection (Lambertian reflection) and two specular reflection components (K-correlation model). Figure 6 reveals excellent fitting curves of the three-component BRDF model to the experimental results. Values obtained from the three-component BRDF model provide information to predict the BRDF behavior of Z302 as a function of wavelength, incidence, and viewing angles for our Monte Carlo ray-trace (MCRT) simulations. The red curves are the three-component BRDF fits of the experimental results. A deconvolution for the three components is illustrated for the glossy, specular, and diffuse reflections. The three reflection components are indicated in the inset.

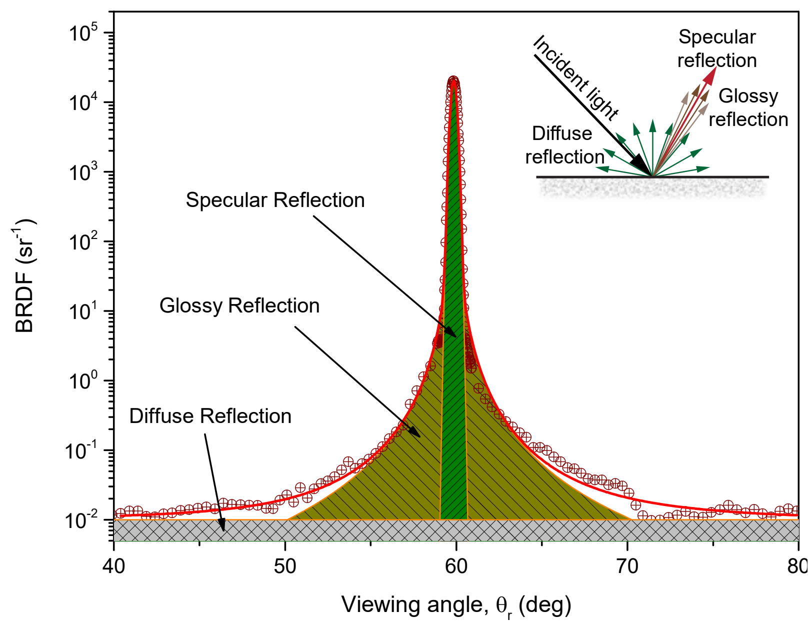

Figure 6. BRDFs measured at 633 nm for the sample coated with Z302 at an incident angle of 60 deg for the *s*-polarization (symbols). The red curves are the three-component BRDF fits of the experimental results. A deconvolution for the three components is illustrated for the glossy, specular, and diffuse reflections. The three reflection components are indicated in the inset.

4. SUMMARY AND CONCLUSIONS

We have employed our custom bidirectional gonio-reflectometer consisting of a two-stage goniometer and various optical elements to investigate the spectral bidirectional reflectance of Z302-coated samples. The sample was illuminated by a 633 nm He-Ne laser and a tunable Ti:Sapphire laser with the wavelength range from 750 to 850 nm, and the signal was measured by a large-dynamic-range photo-detector. The measured BRDFs of the Z302 layer vary in magnitude and shape with viewing angle. We have used a BRDF model consisting of diffuse, glossy, and specular components to explain the experimental results and to mimic scattering processes in Z302 layers. The model is now available for use in simulating the performance of any optical instrument whose surfaces are coated with Z302.

ACKNOWLEDGEMENTS

The authors gratefully acknowledge the financial support of this effort by the Climate Sciences Branch of the Science Directorate of NASA's Langley Research Center.

REFERENCES

[1] Harvey, J. E. , Vernold, C. L., Krywonos, A. and Thompson, P. L., "Diffracted radiance: a fundamental quantity in nonparaxial scalar diffraction theory," Appl. Opt. 38 (31), 6469-6481 (1999).

[2] Prokhorov, A. and Prokhorova, N. I., "Application of the three-component bidirectional reflectance distribution function model to Monte Carlo calculation of spectral effective emissivities of nonisothermal blackbody cavities," Appl. Opt. 51(33), 8003-8012 (2012).

[3] Bailey, A. W., Early, E. A., Keppler, K. S., Villavicencio, V. I., Kennedy, P., Thomas, R. J., Zohner, J. J. and Megaloudis, G., "Dynamic bidirectional reflectance distribution functions: Measurement and representation," J. Laser Applications 20(1), 22-36 (2008).
[4] Z302 material, "*https://www.chembar.com/product/lord-aeroglaze-z302-absorptive-polyurethane-black/"*.
[5] Snail, K. A., Brown, D. P., Costantino, J., Shemano, W. C., Schmidt, C. W., Lynn, W. F., Seaman, C. L. and Knowles, T. R., "Optical Characterization of Black Appliques," Proc. of SPIE 2864, 465-474 (1996).
[6] Shirsekar, D., Wang, Y., Mahan, J. R., Priestley, K. J. and Vinh, N. Q., "Bidirectional reflectance measurement of black absorber layers for use in optical instrument design," Proc. of SPIE 10743, 1074303 (2018).
[7] Shirsekar, D., Vinh, N. Q., Wang, Y., Mahan, J. R. and Priestley, K. J., "Design and demonstration of an automated bidirectional reflectometer for low-reflectivity optical coatings," 4th Thermal and Fluids Engineering Conference in Las Vegas, 27537 (2019).
[8] Mahan, J. R., Walker, J. A. and Stancil, M. M., "Bidirectional reflection effects in practical integrating spheres," Appl. Opt. 54(30), 8951-8956 (2015).
[9] Mahan, J. R., Vinh, N. Q., Ho, V. X. and Munir, N. B., "Monte Carlo ray-trace diffraction based on the Huygens-Fresnel principle," Appl. Opt. 57(18), D56-D62 (2018).
[10] Mahan, J. R., Vinh, N. Q. and Priestley, K. J., "An application of the Monte Carlo ray-trace method with bidirectional reflection," 3rd Thermal and Fluids Engineering Conference in Fort Lauderdale Florida, 22038, (2018).
[11] Mahan, J. R., [The Monte Carlo Ray-Trace Method in Radiation Heat Transfer and Applied Optics.] Wiley, (2018).
[12] Ono, A., "Calculation of the Directional Emissivities of Cavities by the Monte-Carlo Method," J. Opt. Soc. Am. 70(5), 547-554 (1980).
[13] Shen, Y. J., Zhu, Q. Z. and Zhang, Z. M., "A scatterometer for measuring the bidirectional reflectance and transmittance of semiconductor wafers with rough surfaces," Rev. Sci. Instrum., 74(11), 4885-4892 (2003).
[14] White, D. R., Saunders, P., Bonsey, S. J., van de Ven, J. and Edgar, H., "Reflectometer for measuring the bidirectional reflectance of rough surfaces," Appl. Opt. 37(16), 3450-3454 (1998).
[15] Hecht, E., [Optics], Fifth edition, Pearson, ISBN 10: 1-292-09693-4 (2017).
[16] Dittman, M. G., "K-Correlation Power Spectral Density & Surface Scatter model," Proc. SPIE 6291, 62910R (2006).